Red to blue upconversion emission of Tm3+ ions in Yb3+doped glass ceramic

Wu Xu, J. P. Denis, G. Özen, A. Kermaoui, F. Pellé et al.

Citation: J. Appl. Phys. **75**, 4180 (1994); doi: 10.1063/1.356002
View online: http://dx.doi.org/10.1063/1.356002
View Table of Contents: http://jap.aip.org/resource/1/JAPIAU/v75/i8
Published by the American Institute of Physics.

Red to blue up-conversion emission of Tm^{3+} ions in Yb^{3+}-doped glass ceramic

Wu Xu,[a] J. P. Denis, G. Özen, A. Kermaoui,[b] F. Pellé, and B. Blanzat
Laboratoire de Physico-Chimie des Matériaux, C.N.R.S., 1, Place Aristide Briand, 92190 Meudon, France

(Received 26 July 1993; accepted for publication 10 December 1993)

A detailed study of the spectroscopic properties of $PbF_2+GeO_2+WO_3$ glass ceramics doped with Tm^{3+} and codoped with Tm^{3+} and Yb^{3+} ions upon 680 nm dye laser light excitation has been made. The absorption, up-conversion emission, excitation, and time-resolved spectra were measured as a function of TmF_3 and YbF_3 concentrations at room temperature. An enhancement of blue emission centered at 478 nm in the codoped sample was observed. The optium concentrations of TmF_3 and YbF_3 for this blue emission are about 0.2 and 15 mol %, respectively. It is suggested that the results are due to energy transfer between Yb^{3+} and Tm^{3+} ions. Measured oscillator strengths and radiative rates for several transitions are compared with calculated values using the Judd–Ofelt theory with reasonable agreement between theory and experiments for sample doped with Tm^{3+} ions.

I. INTRODUCTION

Glass ceramics doped with rare-earth ions are attractive because they are good up-conversion luminescence materials.[1,2] In addition, they show a high transparency from the UV to the IR and relatively high concentrations of trivalent rare-earth ions can be introduced into the host. Malta *et al.*[3] have investigated the up-conversion process for blue emission of Tm^{3+} ions and energy transfer between Yb^{3+} and Tm^{3+} ions under infrared excitation in PbF_2+GeO_2:Yb_2O_3, Tm_2O_3 compounds. The process was related to a three-photon absorption for blue ($^1G_4 \rightarrow {}^3H_6$) emission band, i.e., energy transfer from the $^2F_{5/2}$ level of Yb^{3+} to $^3H_4$, $^3F_4$, and $^1G_4$ levels of Tm^{3+} ions, respectively. Recently, up-conversion of red light into blue light in fluoride glasses doped with Tm^{3+} ions has been reported.[4–6] This indicates that because the blue emission might result from a two-photon absorption process, the efficiency of up-conversion is higher. We[7,8] have reported the enhancement of blue emission of Tm^{3+} ions is due to the energy transfer upon red excitation in the fluoride glasses and glass ceramics.

In this work, the properties of blue up-conversion emission of Tm^{3+} ions and energy transfer between Yb^{3+} and Tm^{3+} ions have been studied as a function of the concentration of YbF_3 and TmF_3 ions in glass ceramics codoped with Yb^{3+} and Tm^{3+} ions pumped with 680 nm at room temperature. The up-conversion mechanism was elucidated. In addition, the measured oscillator strengths and radiative rates for several transitions of Tm^{3+} ions were compared with calculated values for a single doped sample. Radiative transition rates for the excited states were determined by using the Judd–Ofelt theory.

II. EXPERIMENTS

The samples used in this work were of the general composition $(20-x/2)GeO_2 + (70-y)PbF_2 + (10-x/2)WO_3 + xYbF_3 + yTmF_3$, where x and y are equal to 0, 8, 10, 15 and, 0.05, 0.1, 0.2, 0.3, respectively. The preparation techniques and detailed composition of the sample have been described elsewhere.[8] On the other hand, the sample doped with Tm^{3+} ions was a glass with good optical properties for all concentrations of Tm^{3+} ions.

The optical-absorption spectrum was recorded by using a Cary 17 spectrophotometer that operates from 320 to 2000 nm. Emission spectra upon 680 nm excitation and excitation spectra from 620 to 700 nm were obtained by using an Ar^+ laser pumped-dye laser (Coherent 5920) using DCM dye.

The visible emission signal was measured with a Jobin-Yvon HR 1000 spectrometer and a R649 Hamamatsu photomultiplier tube. The intensity of exciting light at the sample position was detected with a Coherent 200 power meter.

The infrared luminescence was analyzed by a Jobin-Yvon H20 infrared monochromator and a photodiode (UDT-DIN 10308-1). For the time-resolved spectra measuments the excitation was provided by a dye laser (DCM) with a duration of 5 ns pumped with a N_2 laser. The signal was detected by a photomultiplier tube (RTC 56TVP) and then analyzed by a PAR 162 boxcar integrator and the output was displayed on a TF-4000 recorder.

III. RESULTS

The absorption spectrum of Tm^{3+} ions for sample doped with 0.1 mol % Tm^{3+} in the range of 320–2000 nm at room temperature is shown Fig. 1. The spectrum consists of seven absorption bands centered at 1724, 1210, 775, 698, 680, 465, and 356 nm corresponding to the absorptions from the ground state $^3H_6$ to the excitation states

[a]Permanent address: Changchun Institute of Physics, Academia Sinica, People's Republic of China.
[b]Permanent address: Laboratory Laser, CDTA 2bd, BP-1017 Alger Gare, Algeria.

 0021-8979/94/75(8)/4180/9/$6.00

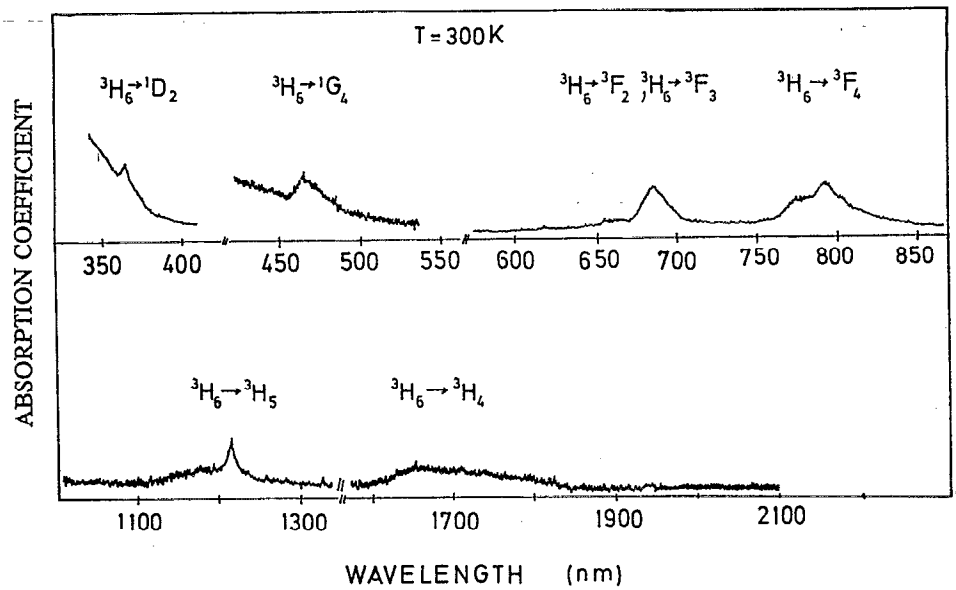

FIG. 1. Absorption spectrum of Tm^{3+} ion in the range of 320–2000 nm for a sample contaiting 0.1 mol % TmF_3 at room temperature.

$^3H_4$, $^3H_5$, $^3F_4$, $^3F_3$, $^3F_2$, $^1G_4$, and $^1D_2$ of Tm^{3+} ion, respectively. This allowed us to determine the energy of the different states of Tm^{3+} ions in the host.

From the absorption spectrum, the oscillator strengths of electronic transition can be calculated expermentally using the following expression:[9,10]

$$f_{\text{meas}}=\left(\frac{mc}{\pi e^2 N}\right)\int 2.303\ \text{OD}(\nu)\,\frac{d\nu}{d}, \tag{1}$$

where m and e are the electron mass and charge respectively, c is the light velocity, N is the number of absorbing ions in the unit volume, ν is the light frequency, $\text{OD}(\nu)$ is the optical density, and d is the thickness of the sample. In this work, d is 1.58 mm.

In the Judd–Ofelt theory,[11,12] the oscillator strength of the $SLJ \rightarrow S'L'J'$ electric dipole transition (at average frequency ν) is given by

$$f_{\text{calc}}=8\pi^2 m\nu(n^2+2)^2 \times \sum_{t=2,4,6} \frac{\Omega_t(\langle SLJ\|U^{(t)}\|S'L'J'\rangle)^2}{[3h(2J+1)9n]}, \tag{2}$$

where n is the refractive index of the host. The Ω_t parameters, known as intensity parameters, are characteristic of each ion-matrix combination and the reduced matrix elements $U^{(t)}$ are not very sensitive to the host (ion environment). In consequence, we used the $U^{(t)}$ element given in Ref. 13. All transitions are assumed to be electric dipolar in nature, except for the $^3H_6 \rightarrow {}^3H_5$ transition which exhibits a non-negligible magnetic dipolar contribution. That transition is neglected in the fitting procedure. From the values of the measured oscillator strengths of the various observed transitions, a least-squares fitting was used to find the Ω_t parameters.

The measured and calculated oscillator strengths are listed in Table I. The intensity parameters for the sample is found to be $\Omega_2=2.17\times10^{-20}$ cm^2; $\Omega_4=0.78\times10^{-20}$ cm^2; $\Omega_6=1.14\times10^{-20}$ cm^2. The quality of the fit is given by the root-mean-square deviation which is equal to 2.68×10^{-7}. This value represents good agreement between measured and calculated oscillator strengths.

The radiative transition probability of an emission transition $(SLJ) \rightarrow (S'L'J')$ is calculated from the following equation:

$$A(J,J')=\left(\frac{64\pi^4 e^2\nu^3}{3h(2J+1)}\right)\left(\frac{n(n^2+2)^2}{9}\right) \times \sum_{t=2,4,6} \Omega_t(\langle SLJ\|U^{(t)}\|S'L'J'\rangle)^2. \tag{3}$$

The radiative lifetime of an excited level SLJ is given by

$$\tau_R=\frac{1}{\Sigma_{J'}A(J,J')}, \tag{4}$$

TABLE I. Measured and calculated oscillator strength of Tm^{3+} ions in the sample at 300 K.

Transition	λ (nm)	Average frequency (cm^{-1})	f_{meas} (10^{-7})	f_{calc} (10^{-7})	Residuals (10^{-7})
$^3H_6 \rightarrow {}^3H_4$	1724	5800	33.59	31.84	1.75
$\rightarrow {}^3F_4$	775	12 903	39.16	40.94	−1.78
$\rightarrow {}^3F_2, {}^3F_3$	687	14 556	54.98	53.15	1.83
$\rightarrow {}^1G_4$	465	21 505	9.86	11.75	−1.89
$\rightarrow {}^1D_2$	356	28 090	28.03	26.95	1.08

$\Omega_2=2.17\times10^{-20}$ cm^2
$\Omega_4=0.78\times10^{-20}$ cm^2 rms$=2.68\times10^{-7}$
$\Omega_6=1.14\times10^{-20}$ cm^2

TABLE II. Calculated and radiative probabilities, radiative lifetimes, and branching ratios of Tm^{3+} ions in the sample.

Transition	Average frequency (cm^{-1})	A ($10^3\ s^{-1}$)	τ_R (ms)	Branching ratios (β)
$^3H_4 \rightarrow {}^3H_6$	5800	0.578	1.73	1.00
$^3F_4 \rightarrow {}^3H_5$	4500	0.128	0.60	0.077
$\rightarrow {}^3H_4$	7103	0.518		0.309
$\rightarrow {}^3H_6$	12 903	1.030		0.614
$^3F_3 \rightarrow {}^3F_4$	1590	0.005	0.15	0.0001
$\rightarrow {}^3H_5$	6909	0.355		0.061
$\rightarrow {}^3H_4$	8693	0.179		0.031
$\rightarrow {}^3H_6$	14 493	5.950		0.908
$^3F_2 \rightarrow {}^3F_3$	322	0.000	0.33	0
$\rightarrow {}^3F_4$	1912	0.152		0.05
$\rightarrow {}^3H_5$	6412	0.478		0.156
$\rightarrow {}^3H_4$	9015	0.874		0.29
$\rightarrow {}^3H_6$	14 815	1.545		0.504
$^1G_4 \rightarrow {}^3F_2$	6690	0.037	0.31	0.01
$\rightarrow {}^3F_3$	7012	0.086		0.025
$\rightarrow {}^3F_4$	8602	0.356		0.104
$\rightarrow {}^3H_5$	13 102	0.846		0.25
$\rightarrow {}^3H_4$	15 705	0.312		0.093
$\rightarrow {}^3H_6$	21 505	1.748		0.517
$^1D_2 \rightarrow {}^1G_4$	6585	0.187	0.035	0.006
$\rightarrow {}^3F_2$	13 275	0.768		0.026
$\rightarrow {}^3F_3$	13 597	0.826		0.028
$\rightarrow {}^3F_4$	15 187	1.668		0.06
$\rightarrow {}^3H_5$	19 690	0.135		0.004
$\rightarrow {}^3H_4$	22 290	14.815		0.512
$\rightarrow {}^3H_6$	28 090	10.510		0.364

where the sum is extended over all the states at energies lower than SLJ. The branching ratios for the different emissions with the same initial level are

$$\beta(J,J') = \frac{A(J,J')}{\Sigma_{J'} A(J,J')}. \tag{5}$$

The results are summarized in Table II for the $^3H_4$, $^3F_4$, $^3F_3$, $^3F_2$, $^1G_4$, and $^1D_2$ levels. The quantum yield η of the emitting level is defined as[14]

$$\eta = \tau_{\exp}/\tau_R, \tag{6}$$

where $\tau_{\exp}$ and τ_R are the experimentally determined and radiative lifetime, respectively. η is presented in Table III for several levels of Tm^{3+} ions.

The up-conversion emission spectrum of the sample doped with 0.2 mol % Tm^{3+} under 680 nm dye laser light excitation in the range 420–520 nm is shown in Fig. 2(a). Two main emission bands centered at 451 and 478 nm are observed. According to the energy-level diagram of Tm^{3+} ion, these emission bands correspond to the $^1D_2 \rightarrow {}^3H_4$ and $^1G_4 \rightarrow {}^3H_6$ transitions respectively; in addition, one other weak emission band can be discerned, viz., the $^1D_2 \rightarrow {}^3H_6$ at 363 nm.

TABLE III. The quantum yields of $^1D_2$, $^1G_4$, and $^3F_4$ levels of Tm^{3+} ions for a sample containing 0.1 mol % TmF_3 at 300 K.

Transition	τ_R (μS)	$\tau_{\exp}$ (μS)	Quantum yields η (%)
$^1D_2 \rightarrow {}^3H_4$ (363 nm)	35	28.5	81.5
$^1G_4 \rightarrow {}^3H_6$ (478 nm)	310	268	86.5
$^3F_4 \rightarrow {}^3H_6$ (779 nm)	600	423	70.5

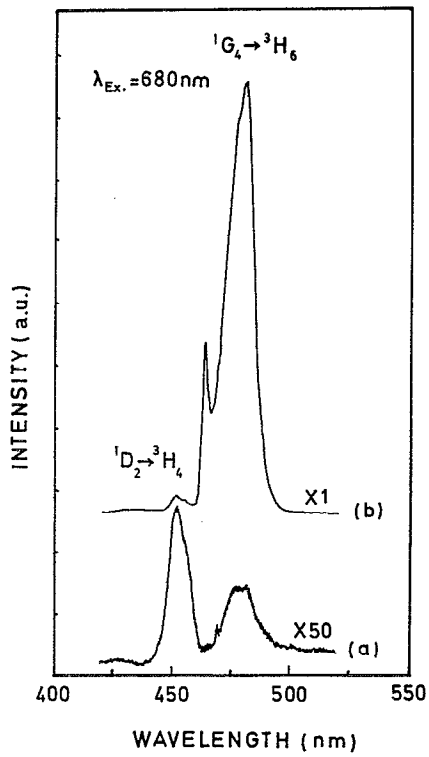

FIG. 2. Blue up-conversion emission spectra of Tm^{3+} ions for both samples upon 680 nm dye laser light excitation at room temperature: (a) sample doped with 0.2 mol % TmF_3; (b) sample codoped with 0.2 mol % TmF_3 and 10 mol % YbF_3.

Figure 2(b) shows the up-conversion emission spectrum of the sample codoped with 10 mol % YbF_3 and 0.2 mol % TmF_3 under the same light excitation. The spectral shape and position of the emission bands are consistent with those obtained for single doped sample, but the intensity of the emission band at 478 nm is much stronger than that obtained in a single doped sample. The intensity ratio of 478 nm emission of the codoped sample to the same emission of the single doped sample is about 240. It is clear that the enhancement of the blue up-conversion emission of Tm^{3+} ions is due to the interaction between Yb^{3+} and Tm^{3+} ions.

In order to select the proper concentration of TmF_3 and YbF_3 in the sample for up-conversion processes, the enhanced blue emission intensity (478 nm) was measured as a function of concentration TmF_3 and YbF_3 under red excitation. Figures 3(a) and 4 show that the dependence of the intensity of blue emission centered at 478 nm on the concentration of TmF_3 and YbF_3 by exciting 680 nm, respectively. It follows from figures that the strongest blue emission occurs when the concentration of TmF_3 and

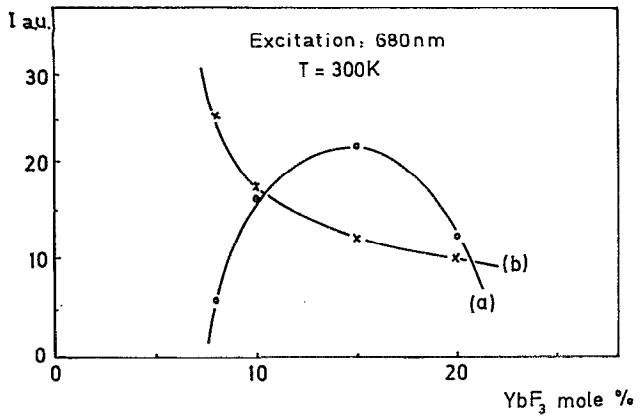

FIG. 3. Dependence of emission intensities of Tm^{3+} ions on the YbF_3 concentration for 0.2 mol % Tm^{3+} under 680 nm light excitation: (a) for 478 nm up-conversion emission ($^1G_4 \rightarrow {}^3H_6$); (b) for 779 nm emission ($^3F_4 \rightarrow {}^3H_6$).

YbF_3 is around 0.2 and 15 mol %, respectively.

In addition to the blue up-conversion emission spectrum, a red emission band centered at 779 nm, which is attributed to the $^3F_4 \rightarrow {}^3H_6$ transition of Tm^{3+} ions was also observed for both compounds (Fig. 5). The intensity of this emission band varies linearly with the 680 nm excitation power. The dependence of the red emission intensity on the concentration of Yb^{3+} ions is presented in Fig. 3(b). The intensity decreases rapidly up to 15 mol % and then the decrease becomes slow above 15 mol %.

The measurement of the excitation spectra in the red region for anti-Stokes emission is important to determine the excitation route in the up-conversion process. The excitation spectra of 478 nm emission for both samples are shown in Fig. 6. There are three excitation bands peaking at 648, 655, and 680 nm in the spectra. These bands are due to the excitation of Tm^{3+} ions from its ground state $^3H_6$ to excited states $^3F_2$ and $^3F_3$, respectively. The inten-

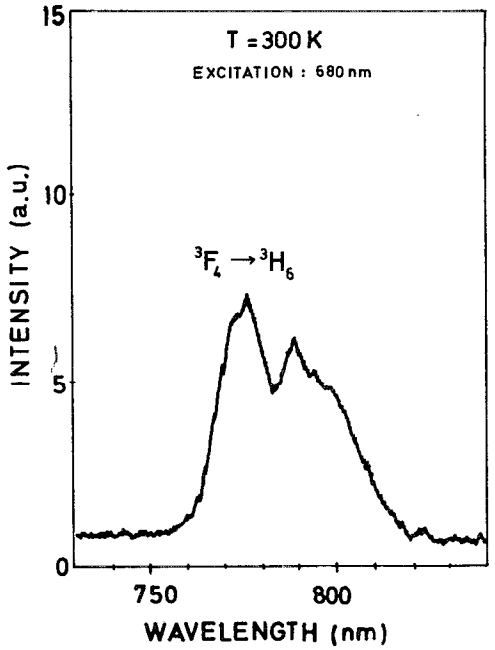

FIG. 5. Red emission spectrum of Tm^{3+} ions for codoped sample under 680 nm light excitation.

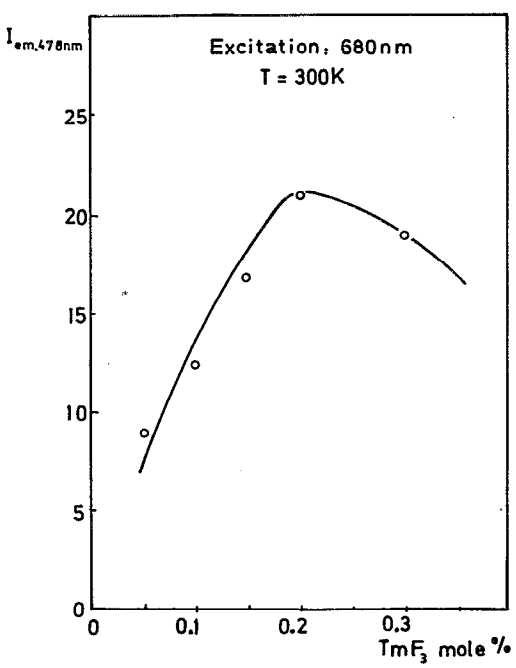

FIG. 4. Dependence of 478 nm enission intensity of Tm^{3+} ions on the concentration of TmF_3 for 15 mol % YbF_3 upon 680 nm light excitation.

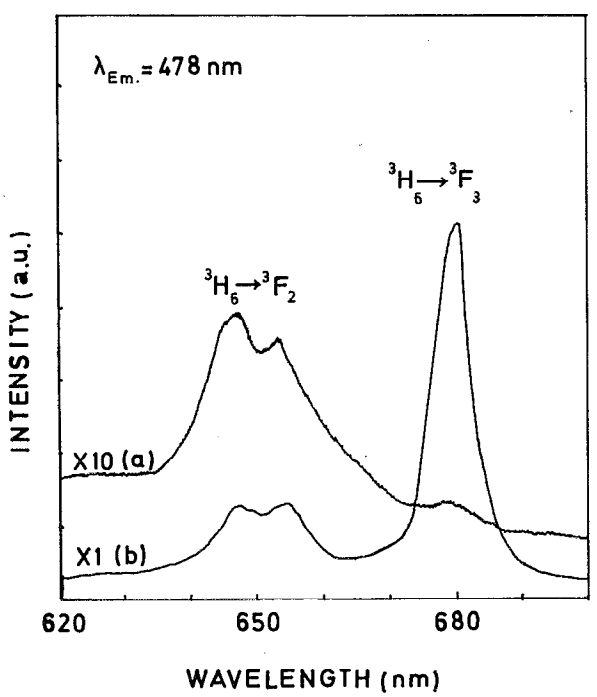

FIG. 6. Excitation spectra for 478 nm up-conversion emission of Tm^{3+} ions in both samples: (a) single doped sample (0.2 mol % Tm^{3+}); (b) codoped sample (10 mol % Yb^{3+} and 0.2 mol % Tm^{3+}).

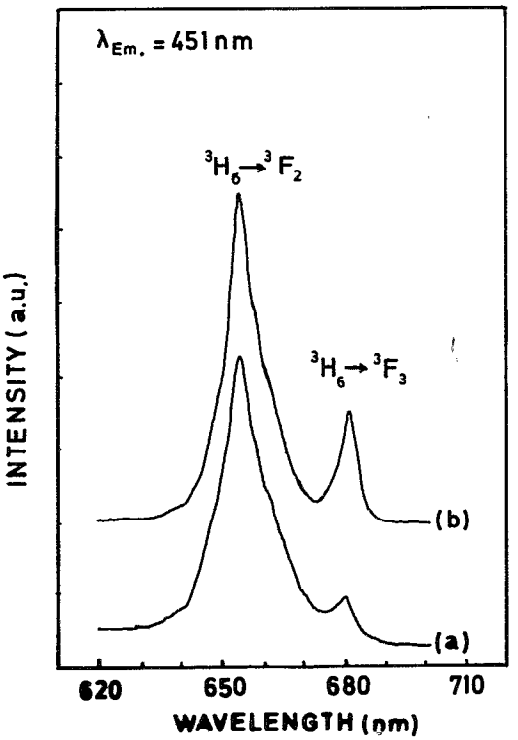

FIG. 7. Excitation spectrum for 451 nm up-conversion emission of Tm^{3+} ions in codoped samples: (a) sample doped with 0.2 mol % TmF_3 and 8 mol % YbF_3; (b) sample doped with 0.2 mol % TmF_3 and 20 mol % YbF_3.

sity of excitation band at 680 nm for codoped sample is much larger than in a single doped sample. This results is in agreement with one of up-conversion emission spectra.

The excitation spectra of the 451 nm emission for codoped samples are given in Fig. 7. The spectra show two bands centered at 655 and 680 nm. For the single doped sample, the intensity of excitation band centered at 680 nm is very weak. In addition, when the concentration of Yb^{3+} ions is changed, the intensity ratio of excitation bands centered at 680 and 655 nm is different. For example, the concentration of YbF_3 ions is increased from 8 to 20 mol %, the ratio varies from 0.13 to 0.32, respectively. This result means that the up-conversion emission for $^1D_2$ level of Tm^{3+} ions is also related to the interaction between Yb^{3+} and Tm^{3+} ions under 680 nm excitation.

The dependence of the intensities of two blue (478 and 451 nm) up-conversion emission bands on the 680 nm light intensity for both samples is reported in Fig. 8. The experimental data have been fit to a straight line. The slopes are found to be about 2 for two blue emissions in single sample. In the double doped sample, the slopes are about 2 and 2.55 for 478 and 451 nm emissions, respectively.

The time-resolved spectra show directly the process of the energy transfer between Yb^{3+} and Tm^{3+} ions. The time-resolved up-conversion spectra of blue (478 and 451 nm) emission bands of Tm^{3+} ions upon 680 nm light excitation for a codoped sample are presented in Fig. 9. The intensities for two blue emission bands increase with the increasing delay time and they reach maximum value at about 150 μs. This phenomenon is absent for single doped sample under same excitation.

It is the best way to confirm the interaction between Tm^{3+} and Yb^{3+} ions by direct measurement of Yb^{3+} emission upon red excitation. Figure 10 represents the emission spectrum of Yb^{3+} ions in a codoped sample under 680 nm excitation. There are two emission bands centered at 945 and 986 nm in the spectrum. According to the energy-level diagram of Yb^{3+} ions, these emissions are due to the transitions from the $^2F_{5/2}$ level to the ground state $^2F_{7/2}$. In addition, these emission bands have been not observed in the sample only doped with Yb^{3+} ions under same excitation.

Figure 11 reportes the 986 nm emission intensity of Yb^{3+} ions versus concentration of TmF_3 in codoped sample under red excitation. It can be seen that the intensity first shows an increase and then a decrease with concentration of TmF_3. The critical concentration of TmF_3 for this emission is about 0.2 mol %.

The excitation spectrum of the 986 nm emission for the codoped sample is shown in Fig. 12. There are two excitation bands centered at 680 and 698 nm in the spectrum. The spectrum has features similar to the absorption spectrum of Tm^{3+} ions due to the $^3H_6 \rightarrow {}^3F_2$ and $^3H_6 \rightarrow {}^3F_3$ absorption (Fig. 1). When the Tm^{3+} ions are excited into the $^3F_2$ or $^3F_3$ levels, the emission of Yb^{3+} ions are observed. It also implies that the emission of Yb^{3+} ions are due to energy transfer from the adjacent excited Tm^{3+} ions upon red excitation for the codoped sample.

IV. DISCUSSION

Two blue emission bands are obtained under 680 nm light excitation and the dependence of the two bands is quadratic on the excitation power for the single doped sample. This means that up-conversion processes involve a two-photon absorption. In the first step, Tm^{3+} ions are directly excited into the $^3F_3$ level upon 680 nm excitation. Then they may relax to the $^3F_4$ and $^3H_4$ levels. Finally, these excited Tm^{3+} ions reach the $^1D_2$ and $^1G_4$ levels by second exciting photon absorption, respectively (Fig. 13). These up-conversion processes are due to an excited state absorption (ESA) process.[5,6]

Tm^{3+} ions are also excited into the $^3F_2$ level upon 655 nm excitation. Then they relax rapidly via $^3F_3$ to $^3F_4$ and $^3H_4$ levels. Blue up-conversion emission bands from $^1D_2$ and $^1G_4$ levels are measured when the second photon is absorbed while the ion is in the $^3F_4$ or $^3H_4$ levels. It is in agreement with excitation spectra of 478 and 451 nm emissions.

When Yb^{3+} ions are codoped into the compound, stronger blue emission, centered at 478 nm, is observed and the emission intensity increases with concentration of Yb^{3+} up to 15 mol %. In addition, the broad excitation band peaking at 680 nm is obtained in the excitation spectrum of 478 nm emission and its intensity follows a square law with the excitation intensity. Moreover the red emission intensity of Tm^{3+} ions ($^3F_4$ level) decreases with concentration of Yb^{3+} ions. On the other hand, the near-infrared emission band of Yb^{3+} ions has been observed in

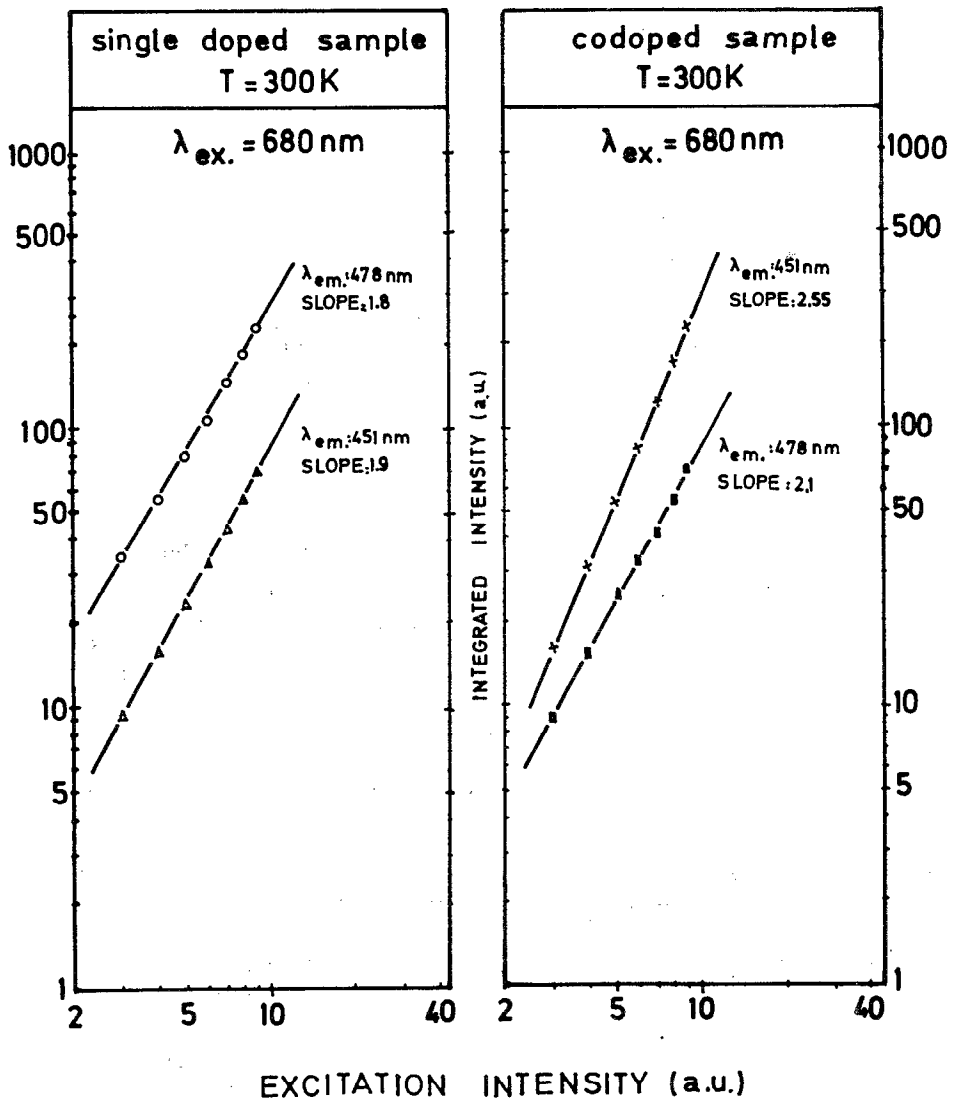

FIG. 8. The blue up-conversion emission intensities vs the excitation power at 680 nm for both samples.

codoped sample under 680 nm light excitation. These phenomenona relate to the interaction between Yb^{3+} and Tm^{3+} ions. We suggest that first excited Tm^{3+} ions in the $^3F_4$ level transfer their energy to nearby Yb^{3+} ions exciting them to the $^2F_{5/2}$ level [$^3F_4(Tm^{3+}) \rightarrow {}^2F_{5/2}(Yb^{3+})$ transfer], then the excited Yb^{3+} ions transfer their energy back to Tm^{3+} ions [$^2F_{5/2}(Yb^{3+}) \rightarrow {}^3H_5$, $^3H_4(Tm^{3+})$ transfer]. This process can excite Tm^{3+} ions into the $^3H_4$ level directly or through the $^3H_5$ level.[15–17] Finally, blue emission from the $^1G_4$ level is observed when the second exciting photon is absorbed while the ions are in the $^3H_4$ level [(1) in Fig. 13]. In addition, the excited Yb^{3+} ions also can transfer energy to Tm^{3+} ions in their $^3F_4$ level, then exciting them into the $^1G_4$ level [$^2F_{5/2}(Yb^{3+}) \rightarrow {}^1G_4(Tm^{3+})$ transfer] [(2) in Fig. 13]. All of these back-energy transfer processes from Yb^{3+} to Tm^{3+} ions enhance the intensity of $^1G_4$ emission in codoped sample. The interaction between Tm^{3+} and Yb^{3+} ions is also confirmed by the fact that there is a clear increase of blue emission intensity of the $^1G_4$ level with delay time in the time-resolved spectra for double doped sample under red excitation.

The dependence of the blue up-conversion emission intensity of the $^1G_4$ level upon the TmF_3 and YbF_3 concentrations has been measured. The blue emission intensity starts decreasing above 0.2 mol % TmF_3 [Fig. 3 curve (a)]. We suggest that quenching of $^1G_4$ level emission is duc to the cross-relaxation processes between two Tm^{3+} ions.[6,9,18] Cross relaxation is an energy transfer process between two Tm^{3+} ions resulting in depopulation of higher excited states. Therefore, cross-relaxation processes decrease the up-conversion emission of the $^1G_4$ level.

The $^1G_4$ level emission can be quenched by four most efficient cross-relaxation processes in Tm^{3+}-ion-doped glass ceramics: ($^1G_4$, $^3H_6$) $\rightarrow$ ($^3F_2$, $^3H_4$); ($^1G_4$, $^3H_6$) $\rightarrow$ ($^3H_5$, $^3F_4$); ($^1G_4$, $^3H_6$) $\rightarrow$ ($^3F_4$, $^3H_5$); and ($^3F_4$, $^3H_6$) $\rightarrow$ ($^3H_4$, $^3H_4$).

On the other hand, the intensity of $^1G_4$ emission increases with YbF_3 concentration up to 15 mol % and then

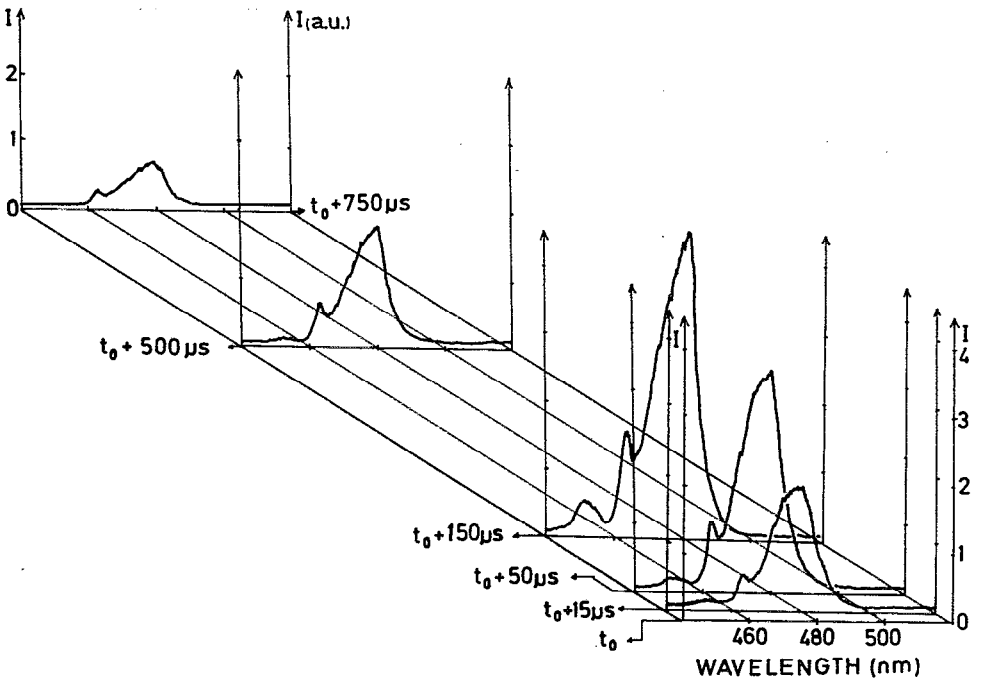

FIG. 9. Time-resolved spectra of Tm^{3+} ions for the sample containing 0.2 mol % TmF_3 and 15 mol % YbF_3 under 680 light excitation.

decreases. The quenching of this emission by YbF_3 concentration may be due to the energy diffusion between Yb^{3+} ions.

Because of the energy transfer from Yb^{3+} to Tm^{3+} ions upon 680 nm light excitation, the obvious increase in emission from the $^1G_4$ level in the time-resolved spectra for the codoped sample was observed (Fig. 9). This result also means that the back-energy transfer process from Yb^{3+} to Tm^{3+} ions is due to the APTE process.[1]

For the codoped sample, the intensity ratio of 680 and 655 nm excitation bands increases as the concentration of Yb^{3+} ions in the excitation spectra of $^1D_2$ level emission (451 nm). In addition, the 451 nm emission intensity I_e varies with excitation intensity I_E following as $I_e \propto I_E^n$, n is about 2.55. This fact means that an extra energy transfer process implying three-photon absorption happens. Moreover, the obvious rising process is measured for this emis-

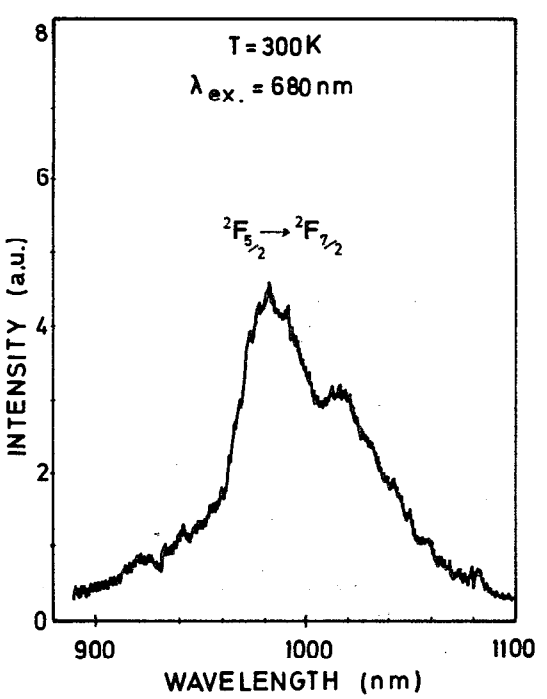

FIG. 10. Emission spectrum of Yb^{3+} ions in the sample coped with 0.2 mol % TmF_3 and 15 mol % YbF_3 upon 680 nm excitation.

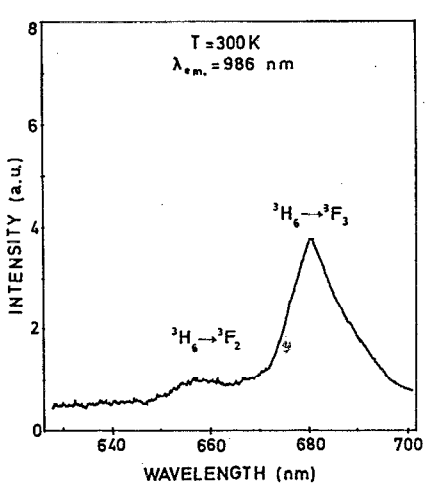

FIG. 11. Dependence emission intensity of Yb^{3+} ions on the TmF_3 concentration for 15 mol % YbF_3 under 680 nm excitation.

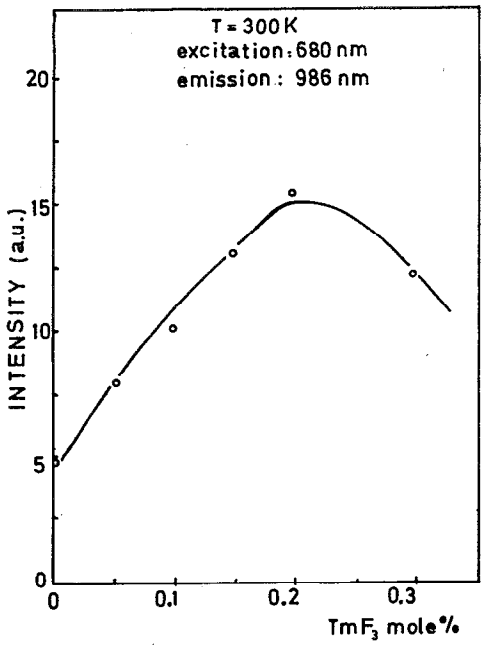

FIG. 12. Excitation spectrum of Yb^{3+} ions in the range of 630–700 nm for the codoped sample.

sion band in the time-resolved spectra upon 680 nm light excitation (Fig. 9). This process has been proposed so that a part of the population of $^1G_4$ level is excited into the $^1D_2$ level by means of energy transfer from excited Yb^{3+} ions [(3) in Fig. 13].

In order to calculate the fluorescence efficiencies for dominant blue (478 nm) of Tm^{3+} ions upon 680 nm light excitation, a comparative method with the standard sample has been used. On the basis of Refs. 19 and 20, the fluorescence efficiency is defined as

$$\eta_u = \eta_s n_u^2 F_u I(\lambda_s) A_s / n_s^2 F_s I(\lambda_u) A_u, \tag{7}$$

where η_u, η_s are efficiencies of unknown and standard, respectively, n is the index of refraction, A is the absorbance, F is the integrated area under the corrected emission spectrum, and $I(\lambda)$ is the relative irradiance of the exciting light at wavelength λ. To determine A, F, and $I(\lambda)$, the detecting system must be calibrated. For the same sample and same excitation power, this equation is reduced to

$$\eta_u = \eta_s F_u I(\lambda_s) A_s / F_s I(\lambda_u) A_u. \tag{8}$$

We have calculated the fluorescence efficiency of 478 nm for up-conversion emission of Tm^{3+} ions in the same sample upon 966 nm light with an absoluted intensity of 16.5 mW/cm^2,[21] and it is 10^{-6}. In the work, this efficiency has been taken for standard efficiency. According to Eq. (8), the fluorescence efficiency of 478 nm up-conversion emissions of Tm^{3+} ions in the sample containing 0.1 mol % TmF_3 and 15 mol % YbF_3 is 8.36×10^{-5} at room temperature when the sample is exciting by 680 nm light with intensity of 16.5 mW/cm^2.

In summary, radiative transition rates for the excited states of Tm^{3+} ions are calculated using Judd–Ofelt theory and intensity parameters are obtained from measured absorption spectrum for the single doped sample.

The stronger blue emission peaking at 478 nm excited with 680 nm dye laser light is observed in glass ceramics codoped with Yb^{3+} and Tm^{3+} ions. The emission intensity increases with concentration of Yb^{3+} ions up to 15 mol % and the quadratic dependence of this emission intensity on the excitation power is obtained. In addition, the emission of Yb^{3+} ions was also observed in codoped sample under 680 nm light excitation. We propose that these experimental results are due to the energy transfer between Yb^{3+} and Tm^{3+} ions.

An additional up-conversion process involving absorption of three photons has been presented for the $^1D_2$ level of Tm^{3+} ions.

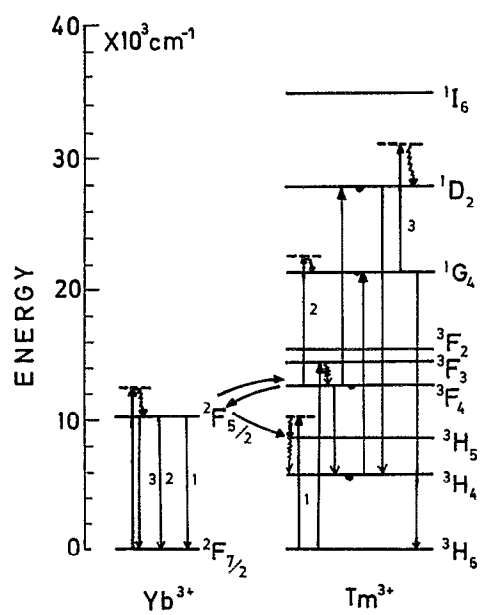

FIG. 13. Energy-levels diagram of Tm^{3+} and Yb^{3+} ions and schematic for up-conversion processes.

ACKNOWLEDGMENTS

The authors are grateful to M. Genotelle for glass ceramics preparation and to Dr. Ph. Goldner for interesting discussions.

[1] F. Auzel, P. Pecile, and D. Morin, J. Electrochem. Soc. **122**, 101 (1973).
[2] F. Auzel, P. A. Santa-Cruy, and C. F. de Sa, Rev. Phys. Appl. **20**, 273 (1987).
[3] O. L. Malta, P. A. Santa-Cruy, G. F. de Sa, and F. Auzel, J. Solid State Chem. **68**, 314 (1987).
[4] J. Y. Allain, M. Monerie, and H. Poignant, Electron. Lett. **26**, 166 (1990).
[5] M. Monerie, T. Georges, P. L. Francois, J. Y. Allain, and D. Neveux, Electron. Lett. **26**, 320 (1990).
[6] E. W. J. L. Oomen, J. Lumin. **50**, 317 (1992).
[7] G. Özen, J. P. Denis, Ph. Goldner, Xu Wu, M. Genotelle, and F. Pellé, Appl. Phys. Lett. **62**, 928 (1993).

[8] Xu Wu, J. P. Denis, G. Özen, Ph. Goldner, M. Genotelle, and F. Pellé, Chem. Phys. Lett. **203**, 211 (1993).
[9] J. Sanz, R. Cases, and R. Alcala, J. Non-Cryst. Solids **93**, 377 (1987).
[10] D. C. Yeh and W. A. Sibley, J. Appl. Phys. **62**, 266 (1987).
[11] B. R. Judd, Phys. Rev. **127**, 750 (1962).
[12] G. S. Ofelt, J. Chem. Phys. **37**, 511 (1962).
[13] N. Spector, R. Reisfeld, and L. Bechm, Chem. Phys. Lett. **49**, 49 (1974).
[14] R. Reisfeld and Y. Eckstein, J. Non-Cryst. Solids **15**, 125 (1974).
[15] F. Auzel, Proc. IEEE **61**, 758 (1973).
[16] D. C. Yeh and W. A. Sibley, J. Appl. Phys. **63**, 4644 (1988).
[17] M. A. Chamarro and R. Cases, J. Lumin. **42**, 267 (1988).
[18] C. Guery, J. L. Adam, and J. Lucas, J. Lumin. **42**, 181 (1988).
[19] A. Kisilev and R. Reisfeld, Sol. Energy **2**, 163 (1984).
[20] R. Reisfeld, Research of The National Bureau of Standards, 1972, Vol. 76 A, p. 613.
[21] W. Xu, J. P. Denis, G. Özen, A. Kermaoui, and F. Pellé, Physics Status Solidi A **141**, 2 (1994).